

Molecular Simulation of the Water Meniscus in Dip-Pen Nanolithography

HYOJEONG KIM, LETON C. SAHA, JOYANTA K. SAHA, AND JOONKYUNG JANG

Department of Nanomaterials Engineering, Pusan National University, Miryang, Republic of Korea

Summary: We report a molecular dynamics simulation of the nanometer water meniscus formed in dip-pen nanolithography (DPN). When an atomic force microscope tip is in contact with a surface, the meniscus is significantly asymmetric around the tip axis. The meniscus as a whole can move away from the tip axis due to surface diffusion. The structure of the meniscus fluctuates and its periphery has a finite thickness as large as 25% of its width. We simulated the transport of nonpolar hydrophobic molecules through a water meniscus. Molecules move on the surface of, not dissolving into the interior of, the meniscus. As a result, an annular pattern forms in DPN. Even if the meniscus is cylindrically symmetric, the molecular flow from the tip and the subsequent pattern growth on the surface are anisotropic at the nanosecond timescale. SCANNING 32: 2–8, 2010. © 2009 Wiley Periodicals, Inc.

Key words: capillary condensation, molecular dynamics simulation, water meniscus, dip pen nanolithography

Introduction

In dip-pen nanolithography (DPN) (Basnar and Wilner 2009; Salaita *et al.* 2007; Nafday *et al.* 2006; Piner *et al.* 1999; Lu *et al.* 2009; Campiglio *et al.* 2009; Giam *et al.* 2009; Sistiabudi and Ivanisevic

2008), water molecules in the air condense as a *meniscus* due to the spatial confinement provided by an atomic force microscope (AFM) tip close to a surface. This confinement-induced *capillary condensation* of water takes place at humidity levels as low as a few percent (Jang *et al.* 2003). The water meniscus is therefore ubiquitous in DPN and AFM experiments under ambient conditions. Most likely, the molecular transport from the tip to surface sensitively depends on the shape and size of the meniscus and the hydrophilicity of the tip. It is speculated that the resolution of DPN relies on the width of the meniscus (Jang *et al.* 2004). The *capillary force* resulting from the meniscus dominates the force exerted on the tip (Israelachvili 1992). Despite the consensus view that the meniscus plays an important role in DPN, our knowledge of the meniscus at the molecular level is far from complete: it is not clear how the meniscus structure and the capillary force depend on the physicochemical properties (e.g. hydrophilicity) and geometrical shapes of the tip and surface (e.g. their roughness and curvature). It is not certain whether 16-mercaptohexadecanoic acid (MHA) is transported via the surface (Nafday *et al.* 2006), through the body (Piner *et al.* 1999) of the meniscus, or both.

Theoretical investigations, which are free of the uncertainties and complications associated with experiments, can fill in the gaps of our molecular picture of the water meniscus and the molecular transport through it. Over the years, we have been using lattice gas (LG) models and grand canonical Monte Carlo simulations to describe the meniscus and the capillary force (Jang *et al.* 2002, 2003, 2004, 2006, 2007). This approach provided molecular insights into the meniscus that are missing from continuum descriptions such as the Kelvin equation (Israelachvili 1992). Our simulations reproduced the typical magnitude of the experimental capillary force and its humidity dependence (Sedin and Rowlen 2000; Asay and Kim 2006; Butt *et al.* 2006; Xiao and Qian 2000). Our LG model, how-

Contract grant sponsor: Korea Research Foundation; Contract grant number: 2009-0071412.

Address for reprints: Joonkyung Jang, Department of Nanomaterials Engineering, Pusan National University, Miryang 627-706, Republic of Korea.
E-mail: jkjang@pusan.ac.kr

Received 28 July 2009; Accepted with revision 27 August 2009

DOI 10.1002/sca.20157

Published online 28 September 2009 in Wiley InterScience (www.interscience.wiley.com)

ever, fails to take into account some features of water molecule, such as its nonlinear geometry and dipole moment. To obtain a fully molecular picture of the meniscus, an atomistic molecular dynamics (MD) simulation is desirable. The recent study of Choi *et al.* 2009 is an example of such a simulation, but its focus was on the capillary force and its dependence on the hydrophilicity of the tip.

Herein, we study the meniscus structure and its role in DPN by using an atomistic MD simulation. We modeled the DPN of octadecanethiol (ODT) grown by a silicon tip on a gold (111) surface. We investigate the structure and stability of a nanometer wide meniscus by calculating and examining its *density profile*. The thickness of the periphery is estimated for the meniscus. We show that the meniscus can be quite asymmetric in the case of a tip in close contact with a surface. We also study the molecular transport from the tip to the surface via the meniscus. ODT molecules initially coated on the tip are found to move on the surface of, not into the body of, the meniscus. Even in the case of a symmetric meniscus, the molecular flow and subsequent pattern growth of ODT on the surface are found to be asymmetric on the nanosecond timescale.

Simulation Methods

Water molecules are modeled using the SPC model (Berendsen *et al.* 1981), which treats each of them as a rigid collection of three point charges (-0.82 on O atoms and $+0.41$ on H atoms). Because of the presence of charges, the water molecules interact through the Coulomb potential. The O atom of water has an additional interaction, resulting from the Lennard-Jones (LJ) potential (Allen and Tildesley 1987),

$$U(r) = 4\epsilon[(\sigma/r)^{12} - (\sigma/r)^6], \quad (1)$$

where σ and ϵ are 0.3166 nm and 0.650 kJ/mol, respectively. The tip is made of Si atoms with LJ parameters, $\sigma = 0.3386$ nm and $\epsilon = 2.447$ kJ/mol (Joseph and Aluru 2006). The surface is made of Au atoms with LJ parameters, $\sigma = 0.2655$ nm and $\epsilon = 4.184$ kJ/mol (Ahn *et al.* 2006). The Si and Au atoms interact with the O atoms through LJ interactions. The LJ parameters, ϵ_{ij} and σ_{ij} , for the interactions between different atomic species i (with σ_i and ϵ_i) and j (with σ_j and ϵ_j) are calculated by using the Lorentz–Bertholet mixing rule (Allen and Tildesley 1987),

$$\epsilon_{ij} = \sqrt{\epsilon_i \epsilon_j} \quad \text{and} \quad \sigma_{ij} = (\sigma_i + \sigma_j)/2. \quad (2)$$

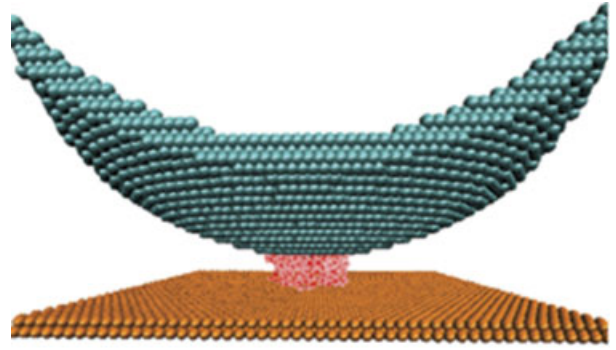


Fig 1. Tip and surface geometries and a representative MD snapshot for a water meniscus. A spherical silicon tip with a radius of 12 nm is separated by 1.5 nm from a Au (111) surface with lateral dimensions of 17 nm \times 17 nm. The water meniscus condensed between the tip and surface is approximately 3 nm wide. The tip and surface, both made of two layers of atoms, contain $12,300$ and $6,352$ atoms, respectively.

The surface geometry consists of the upper two layers of the Au (111) surface (Fig. 1) with a lateral width of 17 nm \times 17 nm. The tip geometry was generated from a simple cubic lattice with a spacing identical to the LJ σ of Si. We first selected two layers of lattice points nearest to a spherical boundary with 12 nm radius. We then removed the part of the layers whose vertical positions are more than 6 nm above the lowest vertical position of the spherical layers. To make the lateral range of the tip identical to that of the surface, we further removed the part of the spherical layers that exceeds the lateral range of the surface (see Fig. 1). The lattice spacing (0.288 nm) for Au (face-centered cubic) is taken from the literature (Ahn *et al.* 2006). The Si tip and Au surface are made of $12,300$ and $6,352$ atoms, respectively. The number of water molecules was set to 370 . Initially, the water molecules are placed regularly in a rectangular box, which fits into the space between the tip and surface. The water molecules formed a meniscus within approximately 50 ps. We varied the tip-surface distance from 0.3 to 1.7 nm (in increments of 0.2 nm) and examined the meniscus structure in each case.

By averaging more than $1,000$ snapshots generated in the simulation, we constructed the density profile, ρ , defined as the average number of O atoms at a given position. We assume that the meniscus has a cylindrical symmetry around the tip axis. Hence, ρ is a function of the *vertical height* from the surface, h , and the *lateral distance* from the tip axis, r . The bin sizes in h and r for the construction of ρ are both 0.35 nm. ρ is normalized so that its highest value is 1 . $\rho(r, h)$ for a fixed h , being a function of r only, is similar to a step function, except that ρ drops rather smoothly, instead of exhibiting a sudden drop, near the meniscus

periphery. The position of the periphery is determined by fitting ρ to the following function,

$$\rho(r, h)|_{h=\text{fixed}} = \frac{1}{2}(\rho_l + \rho_g) - \frac{1}{2}(\rho_l - \rho_g) \tanh \left[\frac{2(r - r_0)}{d_s} \right], \quad (3)$$

where d_s and r_0 are the thickness and location of the periphery, respectively. We used the Levenberg–Marquardt fitting method (Press *et al.* 1996) to determine ρ_l , ρ_g , d_s , and r_0 .

We simulated the molecular transport through the meniscus as follows. The tip is hemispherical with a radius of 10 nm and is separated from the surface by a distance of 2 nm. 8,142 Si atoms are carved out from the same cubic lattice as that described above. We use a coarse-grained model, which treats ODT as a nonpolar spherical LJ atom with $\epsilon = 5.24$ kJ/mol and $\sigma = 0.497$ nm. The same model was used in our previous simulations (Ahn *et al.* 2006; Heo *et al.* 2008). The Au (111) surface is identical to that described above, except that in this case it is laterally bigger (made up of 13,924 atoms). We first put 744 ODT molecules near the tip without the surface and ran the MD simulation for 1 ns using an LJ ϵ value of the tip four times greater than its original value. ODT molecules then spontaneously adhered to the tip, due to their increased attraction to it. We then recovered the original ϵ value for the tip and ran the simulation for another 1 ns. Most of the ODT molecules remained attached to the tip. Next, we added the surface below the tip and put 492 water molecules into the empty space between the ODT-coated tip and surface. By fixing all the molecules except water, we ran a 1 ns simulation for the formation of the water meniscus. Finally, we allowed both the water and ODT molecules to move and observed how the ODT molecules flow from the tip to the surface for 1 ns. Here, we decreased the ϵ value for the tip by four times so that ODT molecules are easily detached from the tip and flow down through the meniscus.

We used the velocity Verlet algorithm with a timestep of 2 fs (Allen and Tildesley 1987). The tip and surface atoms were held rigid. The temperature was set to 300 K using the Berendsen thermostat (Berendsen *et al.* 1984). The internal structure of the water molecules was held rigid using the SETTLE algorithm (Miyamoto and Kollman 1992). The MD simulation methods were implemented utilizing the GROMACS package (Lindahl *et al.* 2001).

Results and Discussion

We investigated the structure of the meniscus by varying the tip-surface distance. Shown in Figure 2 are the contour plots of the density profiles for tip-surface distances of 0.9 (a), 1.1 (b), 1.3 (c), and

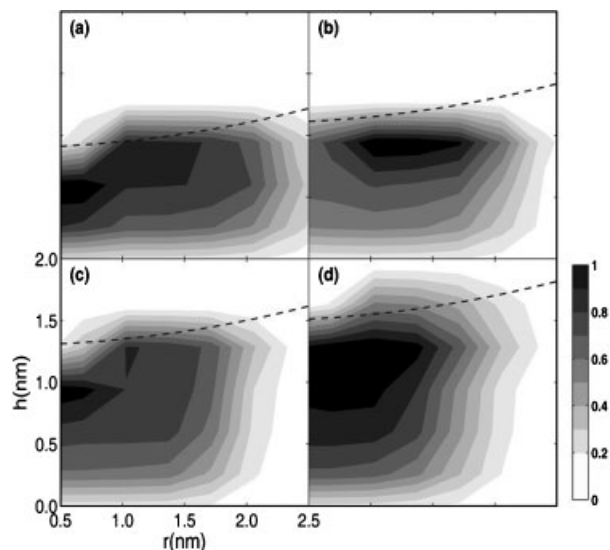


Fig 2. Density profile of water meniscus for various tip-surface distances. The density is contour plotted as a function of the lateral distance from the tip axis, r , and the vertical distance from the surface, h . We used various distances between the tip (Si) and surface (Au), viz. (a) 0.9 nm, (b) 1.1 nm, (c) 1.3 nm, and (d) 1.5 nm. The boundary of the tip is drawn as a dashed line and the surface is located at $h = 0$. The horizontal and vertical axis scales drawn in the lower left panel apply to all the panels.

1.5 (d) nm. Overall, the density decreases from 1 to 0 as r moves away from the tip axis ($r = 0$). For the tip-surface distance of 1.1 nm (b), however, the lateral position of the maximal ρ is not located on the tip axis, $r = 0$, but is separated from the axis by roughly 1.25 nm. This is due to the fact that the meniscus has diffused over the surface as a whole. The common notion that the meniscus positions its center on the tip axis is not necessarily true. In previous LG simulations (Jang *et al.* 2002, 2004), densities above (below) 0.5 are taken to represent the liquid (gas). Here also, we assume that the liquid has a ρ value above 0.5 and that a meniscus is a collection of positions with ρ values above 0.5. Figure 2 shows that the meniscus narrows in width as the tip retracts from the surface. The sizeable spacings between the contour lines indicate that the liquid-to-gas transition in the density profile is rather smooth. This contrasts with a macroscopic meniscus with a sharp transition from liquid to gas at its periphery.

The density profile shown in Figure 2 illustrates the finite thickness of the periphery of the meniscus. This finite thickness is ascribed to the fluctuation of the meniscus as its width narrows (Jang *et al.* 2004). We estimate the thickness of the periphery as follows. For each panel of Figure 2, we fix h to the value corresponding to the horizontal line passing through the maximum of $\rho(r, h)$. The density for h fixed in such a way is a function of r only and is

drawn as circles in Figure 3. We then fitted the density by using the hyper-tangent function described in the Simulation Methods and drew it as solid lines in Figure 3. The fitted liquid densities, ρ_{ℓ} , are 1.00 (a), 0.84 (b), 0.91 (c), and 0.96 (d), and the gas densities $\rho_{g,s}$ are all zero. The corresponding meniscus widths, $2r_{0s}$, are 3.25 nm (a), 3.96 nm (b), 3.30 nm (c), and 3.40 nm (d). The thicknesses of the periphery, $d_{s,s}$, are 0.66 nm (a), 0.46 nm (b), 0.78 nm (c), and 0.75 nm (d), ranging from 12 to 24% of the meniscus widths, $2r_{0s}$. Previously, this ratio was taken to quantify the stability of the meniscus: menisci with ratios of 10% or below were considered to be stable (Jang *et al.* 2004). No meniscus in Figure 3 is stable according to this criterion.

The density profiles in Figure 2 were obtained by assuming the cylindrical symmetry of the meniscus around the tip axis (so that it is a function of r and h only). In the simulation, the shape and size of the meniscus constantly change. Each snapshot of the simulation often deviates from a cylindrically symmetric meniscus. Also, the meniscus as a whole can diffuse on the surface. Figure 4 plots the simulation snapshots of the menisci (top view, taken at 10 ns) for tip-surface distances of 0.3 (a), 0.7 (b), 1.1 (c), and 1.5 (d) nm. At the shortest tip-surface distance of 0.3 nm (a), water molecules do not exist in the region where the tip nearly contacts the surface, resulting in a crescent shape when viewed from the top. The two small droplets shown in the figure are attached to the tip and surface, respectively. In this case, small independent droplets spontaneously separated themselves from the meniscus. As the tip-surface distance increases to 0.7 nm (b), the meniscus becomes more compact and roughly

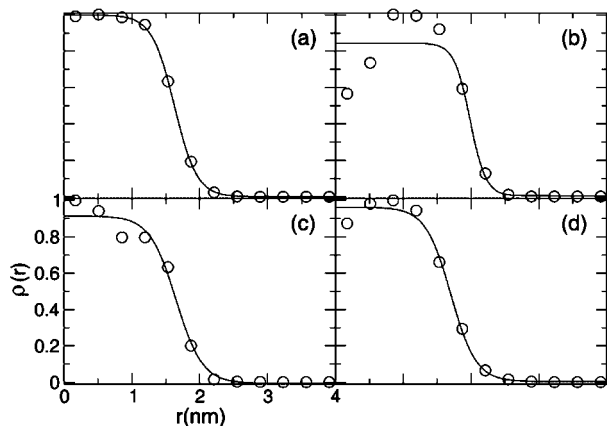


Fig 3. The meniscus density at a fixed height and its nonlinear fitting. For each panel of Figure 2, the density profile, ρ , at a fixed h is drawn as a function of the lateral distance from the tip axis, r (open circles). The fitting results are drawn as solid lines. The horizontal and vertical axis scales drawn in the lower left panel apply to all the panels.

circular. As the tip retracts further away from the surface (c and d), the meniscus keeps shrinking in terms of its lateral size (but its height increases). At the largest tip-surface distance (d), the meniscus is nearly ellipsoidal. The meniscus becomes laterally denser as the tip retracts from the surface. Presumably, the asymmetric menisci shown in Figure 4 would cause the molecular flow in DPN to be anisotropic, especially for a tip in close contact with a surface.

We studied how the meniscus affects the molecular transport from the tip to the surface. ODT molecules are coated on a silicon tip, which is 2 nm above an Au (111) surface (see Simulation Methods for details). Figure 5 shows three consecutive snapshots for molecules flowing down from the tip to the surface. The side and top views of each snapshot are shown on the left (a, c, and e) and right (b, d, and f), respectively. In the top view, the tip and water are excluded for the clear visualization of the ODT molecules. Figures 5(a, c, and e) illustrate the fact that ODT molecules flow down by moving on the surface of the meniscus. No ODT molecules dissolved into the interior of the meniscus. Our spherical ODT molecule is nonpolar so that it interacts only with water molecules through the LJ interactions. The ODT molecule is hydrophobic in the sense that the ODT-water attraction (with LJ $\epsilon = 1.84$ kJ/mol) is smaller than the ODT-ODT

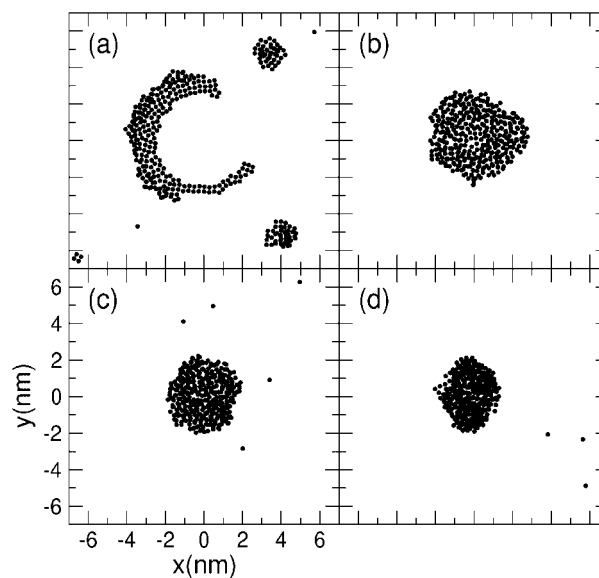


Fig 4. Snapshots of the water menisci at different tip-surface distances with a Si tip and Au surface. Each snapshot is viewed along the tip axis (perpendicular to the surface). Only O atoms are shown (as dots), and the length is in units of nm. Various tip-surface distances are used, viz. (a) 0.3 nm, (b) 0.7 nm, (c) 1.1 nm, and (d) 1.5 nm. The horizontal and vertical axis scales drawn in the lower left panel apply to all the panels.

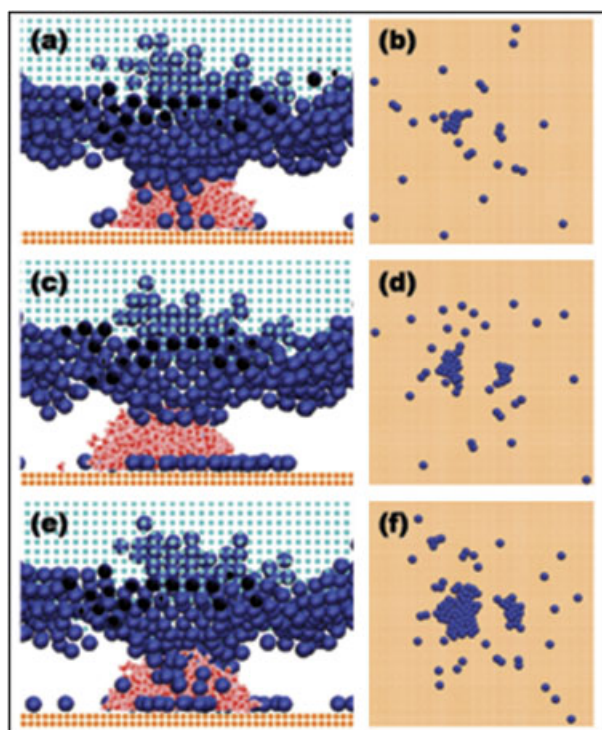


Fig 5. Molecular transport from the tip to the surface via a water meniscus. The side and top views of the snapshot at a given time are drawn in the left and right panels, respectively. Snapshots are taken at three consecutive times of 350 (a and b), 700 (c and d), and 1,000 (e and f) ps. In the side view snapshots (a, c, and e), the Si tip and Au (111) surface are both drawn as dots and the ODT molecules as spheres. Only the ODT molecules near the bottom of tip are shown. A water meniscus connects the tip and surface. The lateral widths of (a), (c), and (e) are all 9 nm. In the top view snapshots (b, d, and f), the tip and water are excluded for the clear visualization of the ODT molecules. The lateral dimensions of surfaces shown in (b), (d), and (f) are all $12.2 \text{ nm} \times 12.2 \text{ nm}$.

intermolecular attraction (with LJ $\epsilon = 5.24 \text{ kJ/mol}$). ODT molecules therefore do not dissolve into the meniscus and opt for moving on the surface of the meniscus. This finding is in similar vein with Nafday *et al.*'s model that amphiphilic molecules are transported at the water–air interface (the surface) of the meniscus (Nafday *et al.* 2006). Our simulation shows that a nonpolar molecule without a hydrophilic group also moves down on the surface of meniscus through the van der Waals (LJ) interaction with water.

Figures 5(b, d, and f) show that the ODT molecular pattern on the surface grows anisotropically and is closer to an annulus than a compact circle. This is in agreement with the annular pattern of DPN using MHA (Nafday *et al.* 2006; Zhang *et al.* 2004). Note that the nearly symmetric meniscus in Figure 5 does not yield an isotropic pattern on the surface. This anisotropy will be further increased if the meniscus structure is asymmetric (as in Fig. 4(a))

or the meniscus laterally diffuses as a whole (as in Figs. 2(b) and 3(b)). In addition, a random coating of molecules on the tip would be expected to increase the anisotropy in the molecular pattern in DPN. It should be mentioned however that the present simulation focused on the short time dynamics ($< 1 \text{ ns}$) of DPN with a diameter less than 10 nm. The anisotropic growth above presumably changes direction with time and the overall pattern growth averaged over a long period of time (experimental timescale, $> 1 \text{ ms}$) will eventually become isotropic, giving rise to a compact circular pattern. In some cases, however (e.g. dodecylamine on a mica surface), the anisotropic growth of the pattern persists even at the experimental time and length scales (Manandhar *et al.* 2003). It is not certain at present whether this is due to the anisotropy in the meniscus or other factors such as the surface anisotropy.

Conclusion

In DPN, a water meniscus naturally forms between the AFM tip and surface under ambient conditions. This meniscus exerts a strong force on the tip and is thought to act as a channel for molecular transport from the tip to the surface. Despite the consensus that the presence of the meniscus fundamentally changes the DPN process, our understanding of the molecular details of the meniscus and its role in DPN remains relatively poor. To improve our molecular picture of DPN, we completed an atomistic MD simulation for a nanometer scale meniscus and the molecular transport through it. The shape of the meniscus fluctuates significantly and its cylindrical symmetry is broken, especially when the tip is in contact with the surface. We also found that the meniscus as a whole sometimes diffuses away from the tip axis. Within our nonpolar spherical model for ODT, molecules flow down to the Au (111) surface by moving on the surface of, rather than by dissolving into the body of, the meniscus. The resulting molecular pattern on the surface is annular. The asymmetric structure of the meniscus presumably introduces anisotropy into the molecular pattern growth on the surface. Even with a cylindrically symmetric meniscus, however, the molecular pattern is found to be anisotropic on the ns timescale. The isotropic and compact dots observed in experiments are likely due to the long-time averaging of the anisotropic pattern growths with different directions.

Admittedly, the present simulation is far from a complete simulation of the molecular processes in DPN. We have not investigated the molecular

detachment from the tip, which is another important process of DPN (Giam *et al.* 2009; Weeks *et al.* 2002). Instead, we took the molecular detachment from the tip as given and focused on the events after the detachment. It is also desirable to consider explicitly the chain structure and the polar head group of ODT molecule. The chains are expected to introduce a molecular entanglement, which will slow down both the detachment from the tip and the flow through the meniscus of ODT molecules. The molecular diffusion on the surface on the other hand is reported to be enhanced by the presence of chains (Mahaffy *et al.* 1997). There is a disparity in size between our simulation and the experimental meniscus, which can be hundreds of nanometers in width (Weeks *et al.* 2005). It needs a further study to check whether the conclusions of our simulation involving hundreds of water molecules remain intact for an experimental meniscus with a number of molecules on the order of 10^9 . We expect some quantitative difference between simulation and experiment, but the qualitative behavior will remain unchanged. It would be also interesting to investigate the dynamics of meniscus formation, which is reported to affect the patterning rate of DPN (Weeks and DeYoreo 2006). The formation of meniscus in simulation was expedited by choosing a liquid-like initial condition for water. If we had used a vapor-like initial condition, the meniscus would have taken a much longer time to form than in this work (~ 50 ps). All these improvements however would require a very long, if possible, simulation time. The current simulation seems a reasonable starting point for an improved modeling of DPN in the future.

Acknowledgements

This work was supported by a Korea Research Foundation Grant funded by the Korean Government (MEST) (No. 2009-0071412).

References

- Ahn Y, Hong S, Jang J: Growth dynamics of self-assembled monolayers in dip-pen nanolithography. *J Phys Chem B* **110**, 4270–4273 (2006).
- Allen MP, Tildesley DJ: *Computer Simulation of Liquids*, Clarendon Press, Oxford (1987).
- Asay DB, Kim SH: Effects of adsorbed water layer structure on adhesion force of silicon oxide nanoasperity contact in humid ambient. *J Chem Phys* **124**, 174712 (2006).
- Basnar B, Wilner I: Dip-pen-nanolithographic patterning of metallic, semiconductor, and metal oxide nanostructures on surfaces. *Small* **5**, 28–44 (2009).
- Berendsen HJC, Postma JPM, van Gunsteren WF, Hermans J: *Intermolecular Forces* (Ed. Pullman B), Reidel, Dordrecht (1981).
- Berendsen HJC, Postma JPM, van Gunsteren WF, DiNola A, Haak JR: Molecular dynamics with coupling to an external bath. *J Chem Phys* **81**, 3684–3690 (1984).
- Butt H-J, Farshchi-Tabrizi M, Kappl M: Using capillary forces to determine the geometry of nanocontacts. *J Appl Phys* **100**, 024312 (2006).
- Campiglio P, Campione M, Sassella A: Kelvin probe force microscopy characterisation of self-assembled monolayers on metals deposited with dip-pen nanolithography. *J Phys Chem C* **113**, 8329–8335 (2009).
- Choi HJ, Kim JY, Hong SD, Ha MY, Jang J: Molecular simulation of the nanoscale water confined between an atomic force microscope tip and a surface. *Mol Simul* **35**, 466–472 (2009).
- Giam LR, Wang Y, Mirkin CA: Nanoscale molecular transport: the case of dip-pen nanolithography. *J Phys Chem A* **113**, 3779–3782 (2009).
- Heo DM, Yang M, Hwang S, Jang J: Molecular dynamics of monolayer deposition using a nanometer tip source. *J Phys Chem C* **112**, 8791–8796 (2008).
- Israelachvili JN: *Intermolecular and Surface Forces*, Academic Press, London (1992).
- Jang J, Ratner MA, Schatz GC: Atomic-scale roughness effect on capillary force in atomic force microscopy. *J Phys Chem B* **110**, 659–662 (2006).
- Jang J, Schatz GC, Ratner MA: Liquid meniscus condensation in dip-pen nanolithography. *J Chem Phys* **116**, 3875–3886 (2002).
- Jang J, Schatz GC, Ratner MA: The capillary force on a nanoscale tip in dip-pen nanolithography. *Phys Rev Lett* **90**, 156104 (2003).
- Jang J, Schatz GC, Ratner MA: How narrow can a meniscus be? *Phys Rev Lett* **92**, 85504 (2004).
- Jang J, Yang M, Schatz GC: Microscopic origin of the humidity dependence of the adhesion force in atomic force microscopy. *J Chem Phys* **126**, 174705 (2007).
- Joseph S, Aluru NR: Hierarchical multiscale simulation of electrokinetic transport in silica nanochannels at the point of zero charge. *Langmuir* **22**, 9041–9051 (2006).
- Lindahl E, Hess B, van der Spoel D: GROMACS 3.0: a package for molecular simulation and trajectory analysis. *J Mol Model* **7**, 306–317 (2001).
- Lu G, Chen Y, Li B, Zhou X, Xue C, *et al.*: Dip-pen nanolithography-generated patterns used as gold etch resists: a comparison study of 16-mercaptohexadecanoic acid and 1-octadecanethiol. *J Phys Chem C* **113**, 4184–4187 (2009).
- Manandhar P, Jang J, Schatz GC, Ratner MA, Hong S: Anomalous surface diffusion in nanoscale direct deposition processes. *Phys Rev Lett* **90**, 115505 (2003).
- Mahaffy R, Bhatia R, Garrison BJ: Diffusion of a butanethiolate molecule on a Au {111} surface. *J Phys Chem B* **101**, 771–773 (1997).
- Miyamoto S, Kollman PA: SETTLE: an analytical version of the SHAKE and RATTLE algorithms for rigid water models. *J Comp Chem* **13**, 952–962 (1992).
- Nafday OA, Vaughn MW, Weeks BL: Evidence of meniscus interface transport in dip-pen nanolithography: an annular diffusion model. *J Chem Phys* **125**, 144703 (2006).
- Piner RD, Zhu J, Xu F, Hong SH, Mirkin CA: “Dip-pen” nanolithography. *Science* **283**, 661–663 (1999).
- Press WH, Flannery BP, Teukolsky SA, Vetterling WT, Metcalf M: *Numerical Recipes in Fortran 90*, Cambridge University Press, Cambridge, New York (1996).
- Salaita K, Wang Y, Mirkin CA: Applications of dip-pen nanolithography. *Nature Nanotechnol* **2**, 145–155 (2007).
- Sedin DL, Rowlen KL: Adhesion forces measured by atomic force microscopy in humid air. *Anal Chem* **72**, 2183–2189 (2000).

- Sistiabudi R, Ivanisevic A: Dip-pen nanolithography of bioactive peptides on collagen-terminated retinal membrane. *Adv Mater* **20**, 3678–3681 (2008).
- Weeks BL, Noy A, Miller AE, De Yoreo JJ: Effect of dissolution kinetics on feature size in dip-pen nanolithography. *Phys Rev Lett* **88**, 255505 (2002).
- Weeks BL, DeYoreo JJ: Dynamic meniscus growth at a scanning probe tip in contact with a gold substrate. *J Phys Chem B* **110**, 10231–10233 (2006).
- Weeks BL, Vaughn MW, De Yoreo JJ: Direct imaging of meniscus formation in atomic force microscopy using environmental scanning electron microscopy. *Langmuir* **21**, 8096–8098 (2005).
- Xiao X, Qian L: Investigation of humidity-dependent capillary force. *Langmuir* **16**, 8153–8158 (2000).
- Zhang H, Elghanian R, Amro NA, Disawal S, Eby R: Dip pen nanolithography stamp tip. *Nano Lett* **4**, 1649–1655 (2004).